Immunity, Vol. 19, 183–192, August, 2003, Copyright ©2003 by Cell Press

Interaction of HLA-DR with an Acidic Face of HLA-DM Disrupts Sequence-Dependent Interactions with Peptides

Achal Pashine,[1,4] Robert Busch,[1,4] Michael P. Belmares,[3,5] Jason N. Munning,[1,5] Robert C. Doebele,[1] Megan Buckingham,[1] Gary P. Nolan,[2] and Elizabeth D. Mellins[1,*]
[1]Department of Pediatrics
[2]Department of Microbiology and Immunology
[3]Department of Chemistry
Stanford University
Stanford, California 94305

Summary

HLA-DM (DM) edits major histocompatibility complex class II (MHCII)-bound peptides in endocytic compartments and stabilizes empty MHCII molecules. Crystal structures of DM have revealed similarity to MHCII but not how DM and MHCII interact. We used mutagenesis to map a MHCII-interacting surface on DM. Mutations on this surface impair DM action on HLA-DR and -DP in cells and DM-dependent peptide loading in vitro. The orientation of DM and MHCII predicted by these studies guided design of soluble DM and DR molecules fused to leucine zippers via their β chains, resulting in stable DM/DR complexes. Peptide release from the complexes was fast and only weakly sequence dependent, arguing that DM diminishes the selectivity of the MHCII groove. Analysis of soluble DM action on soluble DR/peptide complexes corroborates this conclusion.

Introduction

Peptide selection by MHCII dictates which antigens are presented to $CD4^+$ T cells. The affinity of peptides for MHCII is important for peptide selection (McFarland and Beeson, 2002). Peptides are held in the MHCII binding groove by two types of interactions. The first involves largely conserved hydrogen (H) bonds between the MHC molecule and the peptide backbone. The second, dependent on peptide sequence and MHCII polymorphism, involves anchor side chains that interact with specificity pockets in the groove. However, these interactions are cooperative, and the contributions of particular interactions depend on the sequence context.

In vivo, peptide loading of MHCII is regulated by accessory molecules (Busch and Mellins, 1996). In the endoplasmic reticulum, nascent MHCII αβ dimers rapidly associate with invariant chain (Ii) to form an $(\alpha\beta)_3Ii_3$ complex. Residues 90–103 of Ii fill the MHCII groove, inhibiting ligand binding. Upon transport to late endosomes, proteases degrade Ii, leaving a nested set of peptides called CLIP (*cl*ass II-associated *Ii p*eptides, Ii residues 81–104) in the groove. CLIP release is required for loading of other peptides and, for most MHCII alleles, requires the action of DM.

DM is a MHCII-like protein that catalyzes exchange of peptides in the MHCII groove. In DM^0 cells, most MHCII accumulate at the cell surface loaded with CLIP; alleles with low CLIP affinity contain other loosely bound peptides. In vitro, DM promotes release of CLIP and other peptides from MHCII, as well as peptide binding to empty molecules and peptide exchange, and prevents inactivation of empty MHCII. DM interacts directly with MHCII, though apparently not with the bound peptide, and may preferentially bind empty MHCII.

Little is known about the structure of DM/MHCII complexes. The interaction depends strongly on anchoring of both molecules in a common membrane or detergent micelle (Busch et al., 1998; Weber et al., 2001). Biochemical studies implicate surfaces with charged and hydrophobic residues (Sloan et al., 1995; Ullrich et al., 1997). We have mapped a lateral, DM-interacting surface on DR that includes acidic and hydrophobic DR residues near the N terminus of the peptide (Doebele et al., 2000). Two possible complementary surfaces on DM were suggested by X-ray structures (Fremont et al., 1998; Mosyak et al., 1998).

How DM alters the shape of the MHCII groove also remains unclear. Similar DM effects were observed for peptide/MHCII complexes that differ in intrinsic stability (Weber et al., 1996), suggesting that DM may disrupt MHCII H bonds with the peptide backbone. However, in other studies, different complexes differ significantly in their susceptibility to DM (Hall et al., 2002). Reduced DM susceptibility has been correlated with optimal P1 anchor/pocket interactions, extended peptide termini, and lack of glycines and prolines in the core peptide (Chou and Sadegh-Nasseri, 2000; Siklodi et al., 1998; Raddrizzani et al., 1999).

Here we have probed the structure of DM/MHCII complexes by mapping residues important for interaction of DM with MHCII. The orientation of the two molecules predicted by mutagenesis was tested by fusing dimerizing leucine zipper (LZ) domains to DM and MHCII molecules. To explore how DM interaction alters the antigen binding groove, we measured peptide release from LZ-stabilized DM/MHCII complexes and analyzed these results in light of our recent findings with soluble DR/peptide complexes exposed to soluble DM (Belmares et al., 2002).

Results

DM Mutants Cause CLIP Accumulation In Vivo

To identify DM residues important for interaction with MHCII, we transduced mutant *DMA* or *DMB* cDNAs into EBV-transformed B cell lines. In one strategy, we mutated candidate residues and introduced mutant cDNAs into recipient cell lines lacking the appropriate endogenous DM gene (9.5.3 and 2.2.93, respectively; Figure 1A, left). Transduced cells were screened for CLIP accumulation, a hallmark of impaired DM action (Figures 1B–1D).

*Correspondence: mellins@stanford.edu
[4]These authors contributed equally to this work.
[5]These authors contributed equally to this work.

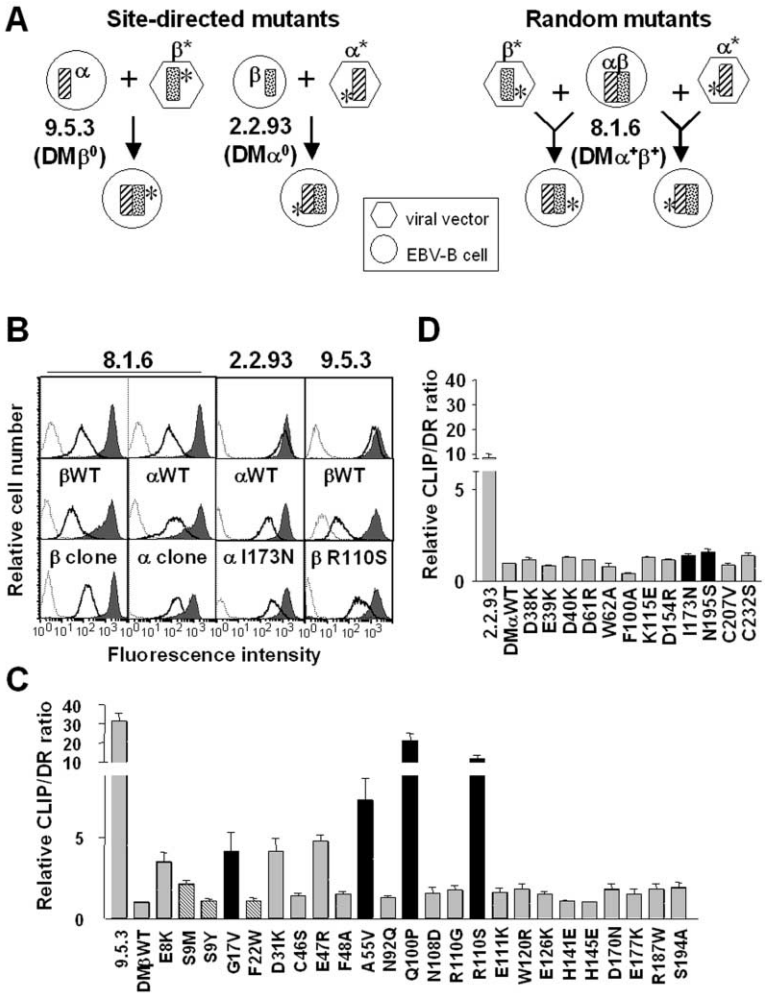

Figure 1. Identification of DM Mutations that Elevate CLIP

(A) Transfection strategies for site-directed and random mutagenesis. (Left) Retrovirus-mediated introduction of mutant (*) *DMB* cDNAs into *DMB*^{0} 9.5.3 cells or mutant *DMA* cDNAs into *DMA*^{0} 2.2.93 cells results in expression of DM$\alpha\beta$ heterodimers with defined point mutations. (Right) Expression of randomly mutagenized *DMA* or *DMB* cDNAs in excess in DM$^+$ 8.1.6 cells allows efficient displacement of the corresponding endogenous wild-type chain during DM dimer assembly.

(B) Assessment of CLIP accumulation by FACS analysis. Fully selected populations of transfectants or untransfected controls were stained with anti-DR (L243; shaded histograms), anti-CLIP (CerCLIP.1; solid lines), or without primary antibody (dotted lines). In 8.1.6 cells, introduction of wt *DMB* (but not *DMA*) diminished CLIP levels, suggesting rescue of excess endogenous α chain. Examples from different experiments are shown.

(C and D) Summary of relative CLIP accumulation in 9.5.3 cells transduced with mutant *DMB* (C) and in 2.2.93 cells transduced with mutant *DMA* cDNAs (D). Background-subtracted CLIP to DR fluorescence ratios were measured as in (B), and the fold increase in this ratio over that for the appropriate wt transfectant is shown for each mutant. Gray bars represent mutants targeting surface-exposed charged and hydrophobic residues. Crosshatched bars indicate mutations filling the vestigial P4′ pocket. Black bars represent site-directed mutants derived from sequencing of high-CLIP clones from the random mutant libraries. Each mutant was analyzed at least twice and usually five to seven times; >2.5-fold changes in CLIP accumulation relative to wild-type were considered meaningful. The dysfunction of mutant βS9M suggested by its slight CLIP elevation was not corroborated in vitro (Figure 2A).

In a complementary strategy, we generated retroviruses carrying *DMB* or *DMA* cDNAs with random mutations. Mutant libraries were expressed in *DMA*$^+$, *DMB*$^+$ 8.1.6 cells, where they competed for one or the other endogenous wild-type (wt) chain (Figure 1A, right). This dominant-negative strategy was aimed at reducing isolation of assembly mutants and was possible because the retroviral promoter drove sufficient expression to displace most of the endogenous wt chain (data not shown). Rare cells with elevated CLIP were cloned and reanalyzed for surface CLIP (Figure 1B). The mutant cDNAs expressed by these clones were sequenced to identify mutations that might impair DM function. cDNAs carrying individual point mutations were then introduced into *DMB*^{0} (9.5.3) or *DMA*^{0} (2.2.93) cells and rescreened for elevated CLIP (Figures 1C and 1D).

Together, these strategies identified seven *DMB* mutations that elevated CLIP to varying extents (βE8K, G17V, D31K, E47R, A55V, Q100P, R110S; Figure 1C). Other mutations failed to confer this phenotype, including βW120R, located on a putative interaction surface (Mosyak et al., 1998; Faubert et al., 2002), as well as mutations (βS9M, S9Y, F22W) designed to fill the vestigial P4′ pocket of DM (Mosyak et al., 1998). None of the *DMA* mutations tested conferred a clear high-CLIP phenotype in 2.2.93 cells (Figure 1D), even though two (αI173N, N195S) originated from the dominant-negative screen. The higher CLIP level in 2.2.93-*DMA* wt cells compared to 9.5.3-*DMB* wt (Figure 1B), likely due to lower DM (Figure 2C), made detection of weak phenotypes more difficult. Intriguingly, one mutation, αF100A, reproducibly conferred a lower level of CLIP than wt *DMA*, suggesting that it improved CLIP release.

To assess the abundance, assembly, and conformational integrity of the mutant DM dimers, we analyzed their expression. Cells harboring βQ100P had low levels of endogenous α chains with an immature glycosylation pattern, suggesting defective chain pairing and/or ER retention (data not shown). Cells expressing αN195S also had low β levels (data not shown), which may explain its modest in vivo CLIP increase (Figure 1D) and initial selection in the dominant-negative screen. In the other mutants, levels of DM heterodimers were measured by DMα immunoblots of DMβ immunoprecipitates (Figures 2A and 2B). Using this semiquantitative assay, we observed normal levels of DM$\alpha\beta$ dimers (less than 1.5-fold different from wt) for mutants βE8K, C46S, R110G and S, and αF100A, less than 3-fold reduced

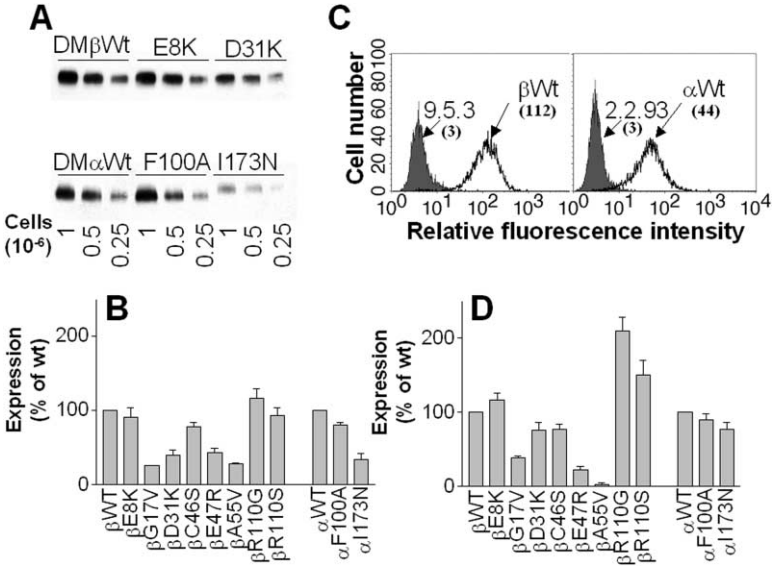

Figure 2. Expression of Mutant DM Molecules

(A) Semiquantitative assay for DMαβ chains. DMβ chains were immunoprecipitated from cell extracts and associated DMα chains were detected by immunoblotting.

(B) Expression of mutant DMαβ dimers, determined by densitometric analysis of blots similar to those shown in (A). Means ± SEM are shown for determinations from dilutions within one experiment. Each mutant was analyzed at least twice with similar results.

(C) Reactivity with the conformation-sensitive mAb, MaP.DM1, measured by intracellular staining and flow cytometry. Fluorescence histograms are shown for *DMB*^{0} 9.5.3 and *DMA*^{0} 2.2.93 cells as negative controls, and for retroviral transfectants carrying wt *DMA* and *DMB* cDNAs.

(D) Expression of MaP.DM1-reactive DM molecules, determined by intracellular flow cytometry as in (C). Expression is normalized to the corresponding wt transfectant; mean ± SEM values of two to twelve independent determinations are shown for each mutant.

levels for βD31K, βE47R, and αI173N, and a 4-fold reduction for βG17V and βA55V. A similar hierarchy was observed by intracellular staining with the conformation-sensitive anti-DMαβ antibody, MaP.DM1. (Figures 2C and 2D). However, MaP.DM1 staining of βR110G and S and αI173N was somewhat higher and staining for βE47R lower than expected based on immunoblots; mutant βA55V lost MaP.DM1 reactivity completely. These discrepancies likely reflect the influence of the mutations on MaP.DM1 binding through conformational distortions or direct disruption of the epitope. Nonetheless, we concluded that all mutants shown in Figure 2 were sufficiently intact to warrant further study.

Mutations Impair Other DM Functions

To evaluate the effects of these mutations in vitro, immunoprecipitated mutant DM molecules were tested for their ability to promote binding of a biotinylated peptide, human chondrocyte glycoprotein 39 $(HCgp39)_{262–276}$, to recombinant DR0402 molecules (or bio-$CLIP_{81–99}$ binding to DR3) (Figures 3A–3F). All *DMB* mutations that elevate CLIP in vivo also impaired DM-dependent peptide binding in vitro. *DMB* mutations that are innocuous in vivo also did not affect DM-dependent peptide binding reactions in vitro (Figures 3B and 3D). This was true for most *DMA* mutations tested as well (Figure 3A). However, for two, the situation was more complex (Figures 3A and 3F). Mutant αI173N entirely lost peptide exchange activity in vitro. The αF100A mutation, which improved CLIP release in vivo, paradoxically abrogated DM-dependent peptide loading in vitro. This mutation may prevent tight peptide binding by stabilizing DM/DR complexes, but this remains to be tested.

To further evaluate mutants with reduced catalytic potential, we tested their function across a range of concentrations (Figures 3C–3F). For βG17V, the reduction in function was approximately proportional to the reduction in input DM (Figure 2 and data not shown), arguing that this mutation did not directly disrupt DM/DR interaction. The profound defect of βA55V was disproportional to the reduced expression of the mutant dimers (Figure 2) but may be due to conformational changes (Figures 2B and 2D). For βE8K, βD31K, βE47R, βR110S, αF100A, and αI173N, expression was only moderately effected (Figure 2), and peptide exchange was not restored at increased concentrations; thus, these mutations likely affect interaction with DR directly (although we cannot exclude subtle conformational effects).

In EBV-B cell lines, ~20%–30% of DM molecules are associated with DO, an MHCII-like molecule that is believed to block DM action (Denzin et al., 1997) but also reported to enhance DM function (Kropshofer et al., 1998). Immunoprecipitated wt DM-DO complexes were inactive in our assay, arguing against a cochaperone role for DO (data not shown). Differential interactions with DO did not explain the functional effects of the DM mutations. Except for the underexpressed αI173N and βE47R mutants, none affected DO steady-state levels (DO accumulation in cells is believed to require association with DM (Liljedahl et al., 1996). Furthermore, a similar fraction of most mutant DM molecules coprecipitated with DO, except for βR110S, which coprecipitated at greatly reduced levels (Figure 3G). Thus, the deleterious effects of the DM mutations on DR/peptide exchange are not due to increased inhibition by DO.

We also examined the effects of some *DMB* mutations on DP. The DP4 allele does not accumulate CLIP in the absence of DM (data not shown). Surface DP is increased ~2-fold by DM transfection (Figure 3H), perhaps due to chaperoning. Mutants βE8K, D31K, E47R, and R110S were impaired in their ability to rescue steady-state DP levels. These mutations thus have parallel effects on DR and DP phenotypes.

Modeling the DM/DR Complex

To examine whether the informative DM mutations identified an interaction surface, we mapped them on the crystal structure of HLA-DM (Figure 4). All six are surface exposed and located on the same lateral face of DM,

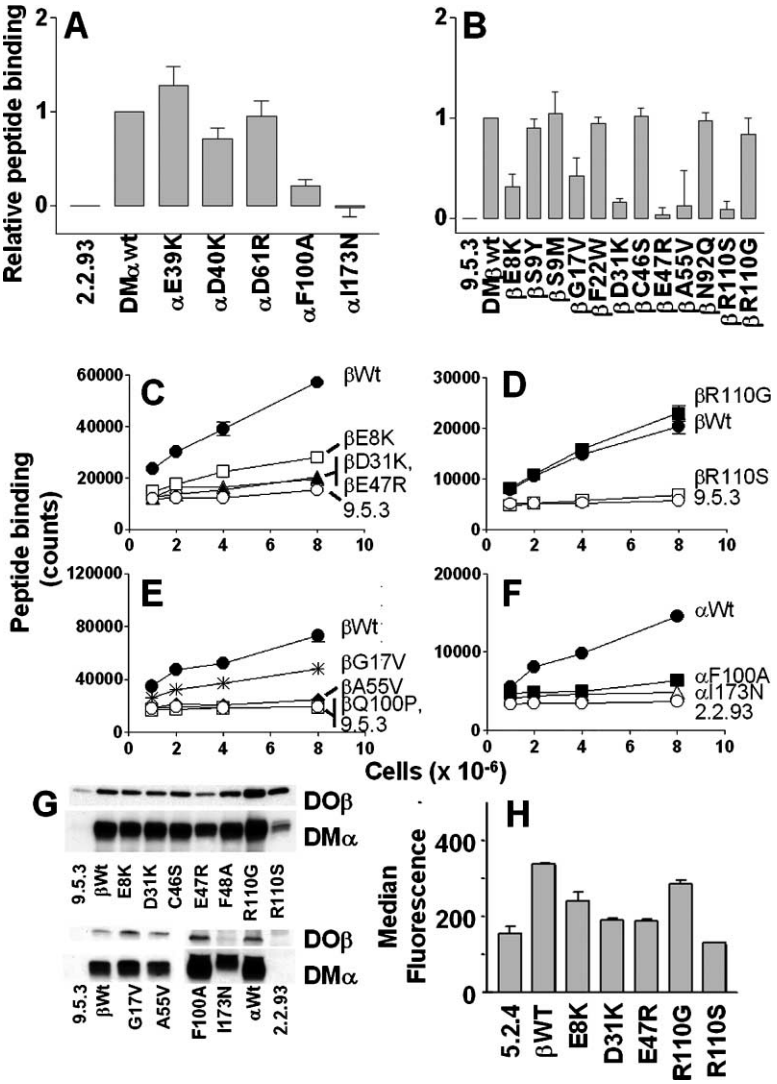

Figure 3. DM Mutations Impair Catalysis of Peptide Binding and DM-Dependent DP Rescue but Not DM/DO Association

(A–F) Wt or mutant DM molecules were immunoprecipitated via their DMβ cytoplasmic tails and tested for catalysis of peptide binding to DR molecules (see Experimental Procedures).

(A and B) Summary of the effects of selected *DMB* (B) or *DMA* (A) mutations on peptide binding. DM was immunoprecipitated from wt or mutant DM transfectants or from DM null cells as controls. Peptide binding was expressed as a fraction of that observed with wild-type DM after subtracting spontaneous peptide/DR binding in the presence of DM null precipitate. Error bars show SEM of two to nine independent experiments.

(C–F) DM immunoprecipitates were prepared from varying numbers of *DMA* (F) or *DMB* (C–E) transfectants and added to peptide binding reactions. Controls without DR gave ≤3000 counts, so the background seen with precipitates from untransfected 9.5.3 or 2.2.93 cells mostly reflects spontaneous peptide binding to DR. Similar results were obtained in at least two independent experiments for each mutant.

(G) Mutant DM molecules stabilize and coprecipitate with DO. Cells harboring mutant DM were subjected to DO immunoprecipitation. Immunoprecipitates were analyzed for DO using DOB.L1 and for associated DM using 5C1.

(H) Effect of *DMB* mutations on surface DP levels. 5.2.4 transfectants with mutant DMB chains were stained with mAb to DP and analyzed by flow cytometry. Error bars show SEM of three independent experiments.

with βE8, D31 and E47 forming part of a conserved acidic cluster (Fremont et al., 1998). In contrast, the mutations whose functional defects appear due to altered expression (βG17V, βQ100P, αN195S) do not map near this face.

The αI173N and βR110S mutations caused addition of extra N-linked glycans at residues αI173 and βN108, respectively (Figure 2A and data not shown). Glycosylation likely is responsible for the profound phenotype of βR110S because βR110G, lacking the glycan, had a normal phenotype. The concave shape of DM's interaction surface is complementary to the convex interaction surface on DR (Doebele et al., 2000).

β Chain LZ Fusions Stabilize the DM/DR Complex

The C termini of the DRβ and DMβ chains are closer to each other in the modeled complex than any other combination of C termini. Thus, to test the model, we employed soluble DR and DM molecules whose β chain C termini were fused, via short spacers, to complementary LZ domains (BaseP1 and AcidP1, respectively; Figure 4). Properly assembled and secreted LZβ-DM and -DR1 molecules were purified (Busch et al., 2002). To assess whether LZ fusion stabilized functional DM/DR complexes, we tested varying amounts of affinity-purified LZβ-DM or soluble DM (sDM) for their ability to promote binding of biotinylated HA (306–318) peptide to LZβ-DR1 or sDR1 molecules at endosomal pH. The need for large amounts of sDM (Figure 5A) or LZβ-DM (Busch et al., 2002) to catalyze peptide binding to sDR1 reflects inefficient interaction of the soluble ectodomains. In contrast, 3000× less LZβ-DM catalyzed peptide binding to LZβ-DR1, indicating that the LZ domain interaction stabilized DM/DR complexes. Some enhancement was also seen when LZβ-DR1 was used as a substrate for sDM. We tentatively attribute this to electrostatic interaction between the positively charged Base-P1 LZ domain on DR1 and the negatively charged epitope tags at the C termini of DMα and β. At neutral pH, the same hierarchy was observed, but catalysis was less efficient. This pH effect suggested that biologically relevant complexes were stabilized and that the LZ domain and DM/DR ectodomain interactions were independent, but did not rule out the possibility that the LZ

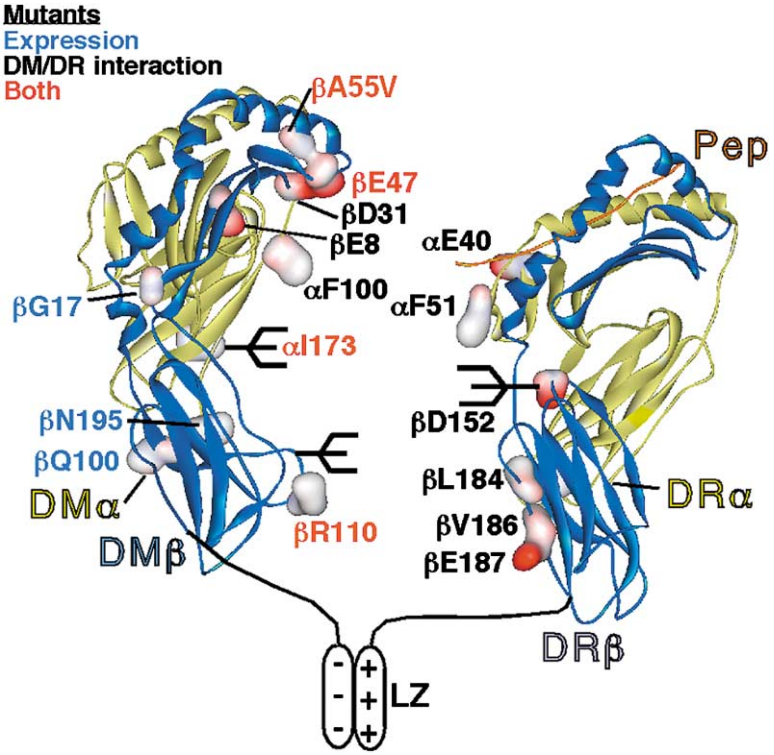

Figure 4. Model of DM/DR Interaction

(Left) Location of mutants, mapped on the crystal structure of DM (Protein Data Bank accession code 1HDM). Mutations were color coded based on their effect on DM expression, DM/DR interaction, or both. (Right) Structure of DR3/CLIP with DM interaction mutants indicated (Doebele et al., 2000). Structures are oriented so as to juxtapose the interacting surfaces. All chains are labeled at their C termini; the DMα C terminus is hidden behind βQ100. LZ domain fusion via β chain C termini is depicted schematically. Molecules were visualized using WebLab Viewer Lite V3.5 (Molecular Simulations Inc., San Diego, CA).

domains constrain the range of orientations available during DM/DR binding.

The model predicted that LZ fusion via the α chain C terminus of DR might stabilize DM/DR complexes less (Figure 4). Indeed, there was little enhancement of LZα-DR1/peptide binding in the presence of LZβ-DM (Figure 5B), although, in the absence of DM, LZα-DR1 molecules bound similar amounts of peptide as did LZβ-DR1 and sDR1 (data not shown). LZα-DR1 also did not share the increased susceptibility of LZβ-DR1 to sDM (Figure 5C). The LZ domain in LZα-DR1 was not inaccessible; a mAb to the AcidP1/BaseP1 LZ dimer coprecipitated LZα-DR1 and LZβ-DM from mixtures of both molecules (Figure 5D). However, zippering via the DRα C terminus appears to destabilize the LZβ-DMαβ dimer because a disproportionately low amount of sDMα was coprecipitated. We concluded that LZα-DR1 allowed assembly with LZβ-DM, but without stabilizing a productive DM/DR complex.

Diminished Selectivity of Rapid Peptide Release from DM/DR1 Complexes

To investigate the effect of DM interaction on peptide release, we formed complexes between aminomethyl coumarin acetic acid (AMCA)-labeled HA and CLIP and LZβ-DR1 and tracked their release in real time. Fluorescence resonance energy transfer (FRET) between tryptophans of DR and the AMCA fluorophore was used to quantify bound peptide (Figure 6; Joshi et al., 2000). In the absence of DM, we found a 200-fold difference in kinetic stability between AMCA-HA and AMCA-CLIP bound to LZβ-DR1 ($t_{1/2}$ = 1 month versus 4 hr; Figure 6A and Table 1). When an equimolar amount of LZβ-DM was added, dissociation was greatly accelerated for the majority of complexes (Figure 6B). Soluble DM without LZ domains has far lesser effects on peptide release at these concentrations (data not shown; Zarutskie et al., 2001), so the rapid release involved LZ-mediated stabilization. Surprisingly, the difference in stability between CLIP and HA was only ~10-fold ($t_{1/2}$ ~10 s versus 2 min), suggesting that DM interaction reduced the selectivity of the antigen binding groove.

To characterize this effect further, we exposed HA and CLIP complexes to varying concentrations of LZβ-DM. With 10-fold less DM, the proportion of LZβ-DM-susceptible complexes remained the same, whereas the off rates of both complexes were reduced (Figure 6C). Thus, LZβ-DM exchanged rapidly between susceptible AMCA-peptide/LZβ-DR1 complexes; otherwise, at most 10% of the complexes would have dissociated, or more complex kinetics would be seen. The ~10-fold difference in LZβ-DM-dependent dissociation between AMCA-CLIP and AMCA-HA was seen at all DM concentrations tested (Figure 6D). A 1:1 molar ratio of DM to complex was sufficient to reach maximal off rates (Figure 6D; Table 1), which presumably represented rates of peptide release from the DM/DR complex. At limiting concentrations, the off rates were proportional to the amount of LZβ-DM. This behavior is consistent with a Michaelis-Menten model, in which LZβ-DM (the enzyme) is in rapid preequilibrium with the AMCA-peptide/LZβ-DR1 complexes (substrates), followed by a rate-limiting peptide release step:

$$\mathrm{DM} + \mathrm{DR1/peptide} \overset{K_M}{\longleftrightarrow} \mathrm{DM/DR1/peptide}$$

$$\overset{k_{cat}}{\rightarrow} \mathrm{DM/DR1} + \mathrm{peptide}. \qquad (1)$$

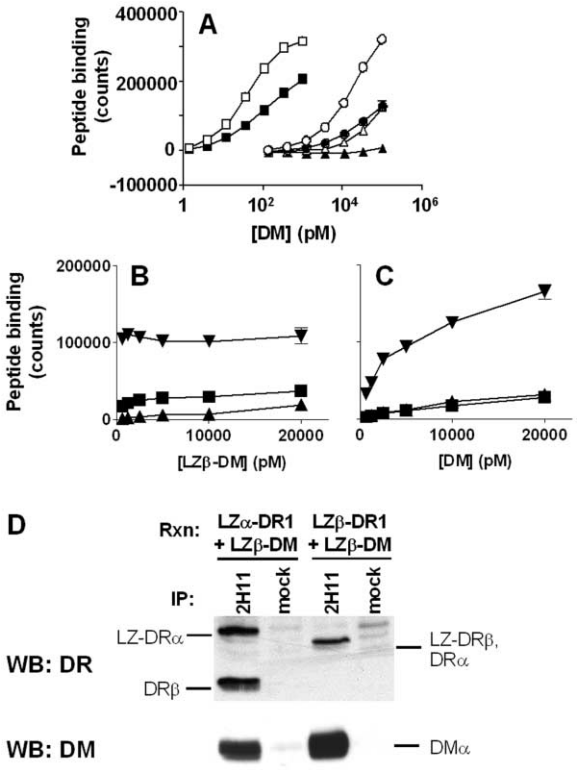

Figure 5. LZ Modification of DR1β and DMβ Stabilizes DM/DR Complexes

(A) Stabilization of physiologic DM/DR1 complexes by β chain LZ fusion. Binding of bio-HA (307–319) to DR molecules in the presence of the indicated doses of DM molecules was measured at pH 4.7 (open symbols) or pH 7.0 (filled symbols). Squares, LZβ-DM and LZβ-DR1; circles, sDM and LZβ-DR1; triangles, sDM and sDR1. Spontaneous peptide binding in the absence of DM (35,000–65,000 counts, depending on pH) was subtracted. The experiment was done twice with similar results.

(B and C) Inefficient stabilization of functional DM/DR complexes by BaseP1 LZ domain fusion via the DRα C terminus. Peptide binding assays were performed at pH 4.7 as in (B), using LZα-DR1, (■), purified sDR1 (▲), or purified LZβ-DR1 (▼). (B) Peptide binding to 10 nM DR molecules in the presence of varying amounts of LZβ-DM. (C) Peptide binding in the presence of sDM. Similar results were obtained in four experiments, using concentrated insect supernatants (matched for DR content) or purified material as a source of LZα-DR1.

(D) LZα-DR1 assembles with LZβ-DM via the LZ domains. LZβ-DM was mixed with LZα-DR1 or with LZβ-DR1 and immunoprecipitated using a mAb against the AcidP1/BaseP1 LZ dimer (2H11), or normal mouse Ig (mock). Precipitates were analyzed by immunoblotting using CHAMP (top, anti-DRα/β) and 5C1 (bottom, anti-DMα). Note that in LZβ-DR1, the α and LZ-fused β chain comigrate. Blotting with SU36 (anti-DMα/β) indicated partial loss of α but not β chain of LZβ-DM from 2H11 coprecipitates with LZα-DR1 (data not shown).

Indeed, when we measured initial off rates for varying concentrations of both complexes in the presence of catalytic amounts of LZβ-DM, good fits to Michaelis-Menten models were observed (Figure 6E). Importantly, k_{cat} values for the peptide/LZβ-DR1 complexes differed by only ≈10-fold and were similar to the off rates measured at equimolar amounts of LZβ-DM (Table 1), consistent with k_{cat} reflecting the rate-limiting peptide release step.

Does the apparent loss of selectivity of the MHCII groove in DM/DR complexes also occur in the absence of LZ domains and with other peptide/DR complexes? Without LZ stabilization, the low affinity of soluble DR or DM ectodomains for each other precluded direct measurement of k_{cat} or of peptide release from 1:1 DM/DR/peptide complexes. Instead, we exploited the fact that when substrate concentrations are low compared to K_M, the rate law simplifies to $k_{obs} = k_{in} + j\ k_{in}$ [DM], where k_{obs} is the observed dissociation rate constant in the presence of DM and j is a concentration-independent measure of DM susceptibility (Weber et al., 1996). If DM has no effect on the selectivity of the antigen binding groove, the rate enhancement by DM, and hence j, should not vary systematically with intrinsic stability. In contrast, if the groove becomes less selective upon interaction with DM, then stability differences between peptide/MHCII complexes should be less pronounced in the presence of DM, and DM susceptibility (j) should decrease as k_{in} increases. We have recently measured peptide release rates for a large number of different peptide/DR complexes in the presence and absence of soluble DM (Belmares et al., 2002). The complexes ranged in intrinsic stability ($t_{1/2}$) from hours to months; they represented four different DR alleles, bound to a large panel of CLIP variants and peptides derived from self- or foreign antigens. In Figure 6F, we show that values of j vary over three orders of magnitude for these complexes. When stratified for high, intermediate, or low intrinsic stability (low, intermediate, or high k_{in}), there was substantial variation in j for each group. Nonetheless, there was a significant trend toward lower values of j for less stable complexes, seen for all four DR alleles (Belmares et al., 2002). We concluded that the ability of DM to diminish the selectivity of peptide release from the MHCII groove is not an artifact of LZ stabilization and appears to be a general feature of DM/MHC II interactions.

Discussion

By mutagenesis, we identified ten individual residues that are critical for normal DM function. While mutants βG17V, βQ100P, and αN195S primarily alter DM assembly or expression, the other residues cluster on or near a common lateral surface of the molecule (Figure 4), implicating this surface in direct or indirect interaction with MHCII molecules during peptide exchange. The design of LZ domain-stabilized DM/DR1 complexes based on this information and the shape complementarity of the candidate MHCII-interacting surface with the DM-interacting face of DR strongly suggest a direct interaction. Precise modeling of the interactions within the DM/MHCII complex remains difficult, however. Mutations that introduce large glycan moieties at the interface (βR110S, αI173N) cannot provide fine structural detail. Mutants βA55V and βE47R may act indirectly, e.g., via nearby acidic residues. Finally, the decreased selectivity of peptide release from the DM/DR complex described here suggests that the conformation of the MHCII groove may be altered more substantially by interaction with DM than was previously appreciated.

Our data agree with available information about the

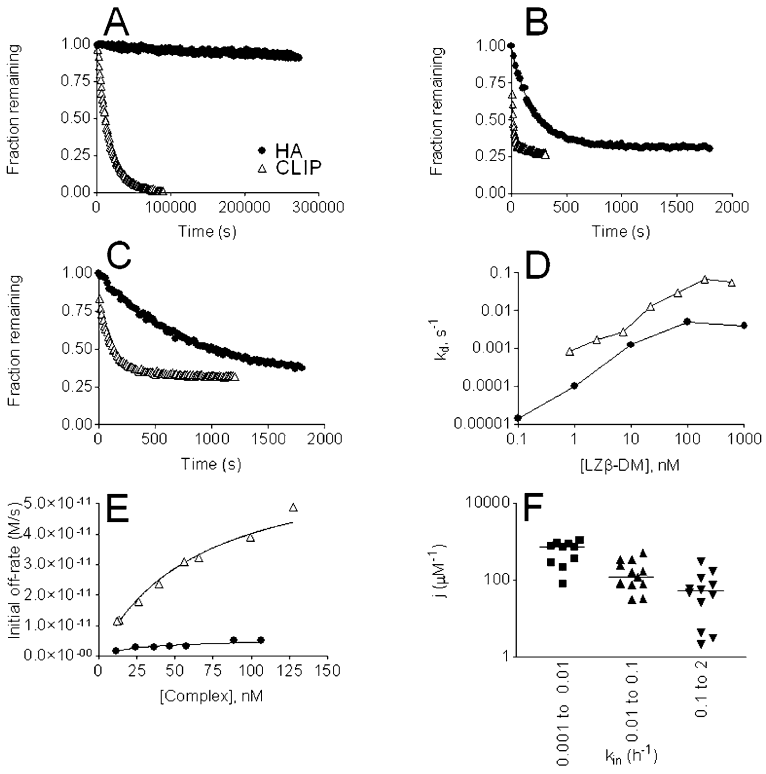

Figure 6. Rapid, Nonselective Peptide Release from DM/DR Complexes

In (A–E), LZβ-DR1 complexes with AMCA-labeled variant HA (closed circles) or CLIP (open triangles) peptides were formed overnight and allowed to dissociate at pH 5.1 in the presence of excess unlabeled competitor peptide. Dissociation was monitored by real-time FRET. Kinetic parameters are summarized in Table 1.

(A) Spontaneous peptide release from LZβ-DR1 (100–200 nM initial complex) in the absence of DM. Lines represent single-exponential fits to the data.

(B and C) Peptide release from LZβ-DR1 (100–200 nM initial complex) in the presence of equimolar (B) or substoichiometric amounts (10 nM; [C]) of LZβ-DM. Some 30% of the complexes (15%–50%, depending on the DR preparation) failed to undergo LZ-dependent peptide release, regardless of the DM concentration. We attribute this to steric inaccessibility of the LZ domain in the resistant subpopulation; immunoblots revealed no significant proteolysis of the LZ domains (data not shown).

(D) Rate constants, k_d, for LZ-dependent dissociation of susceptible AMCA-HA/LZβ-DR1 (100 nM) and AMCA-CLIP/LZβ-DR1 (200 nM) complexes in the presence of varying amounts of LZβ-DM.

(E) Michaelis-Menten kinetics. Varying concentrations of peptide/LZβ-DR1 complexes were allowed to dissociate with or without 1 nM LZβ-DM. Initial LZβ-DM-catalyzed off rates were plotted after subtraction of background dissociation without LZβ-DM.

(F) Susceptibility of 35 different soluble peptide/DR2 and DR4 complexes to soluble DM. Dissociation was measured with or without soluble DM (Belmares et al., 2002). Complexes were grouped according to their intrinsic stability, as measured by k_{in}, the dissociation rate constant in the absence of DM. DM susceptibility was measured by the concentration-independent parameter, $j = (k_{obs}/k_{in} - 1)/[DM]$, where k_{obs} is the dissociation rate constant measured in the presence of a given amount of DM. Horizontal lines indicate medians. The trend toward decreased j at higher k_{in} across all groups is significant ($p < 0.0001$ by one-way ANOVA with posttest for linear trend for log j) and does not vary strongly by DR allele (Belmares et al., 2002). One complex with high intrinsic stability and atypical DM resistance was omitted from this analysis.

DM/MHCII interaction. Informative mutants lie along the length of DM, consistent with the elongated shape of the complementary face of DR (Doebele et al., 2000) and with a requirement for membrane anchoring for optimal DM/MHCII interaction (Weber et al., 2001). Studies using a peptide tethered to βC46 on the same face of DM (Stratikos et al., 2002) also agree with the orientation of the complex proposed here. Both site-directed and random mutagenesis of DMα and β failed to identify additional binding sites, suggesting that DM has one binding site for a single MHCII molecule, as previously proposed based on molecular sizing (Sanderson et al., 1996). The mutations that alter DM function corroborate prior evidence for charge and hydrophobic interactions between DM and DR (Doebele et al., 2000; Ullrich et al., 1997; Sloan et al., 1995).

Protonation of acidic residues on both DM and DR at endosomal pH may relieve charge repulsion and may allow greater exposure of hydrophobic residues and/or formation of hydrogen bonds at the interface. Complexes of MHC molecules with other ligands share some of the features described here for DM. Examples include a similarly located acidic cluster at the F_c contact surface of rat neonatal F_c receptor (Burmeister et al., 1994) and the concave surfaces of classical MHC class I molecules interacting with CD8 (Gao et al., 1997) and Ly49 (Tormo et al., 1999).

The DM mutations had effects on DR and DP, largely without affecting interactions with DO. This interaction, which is more difficult to disrupt with detergents (Liljedahl et al., 1996), may also be less sensitive to DM mutations. Nonetheless, the ability of the *DMB* glycosylation mutant to diminish DM/DO interaction supports the contention that the binding sites are overlapping.

The rates of peptide release from DM/DR1 complexes suggest substantial changes in the DR1 groove induced by DM binding. Despite modest turnover numbers, DM enhances peptide release by 3–5 orders of magnitude (Table 1), more than typically seen upon disruption of the conserved H bond network by mutation (McFarland and Beeson, 2002). Due to cooperativity effects, disruption of H bonds has the greatest effect on unstable MHCII/peptide complexes, whereas the opposite is true for DM action: the greatest rate enhancements are seen for the most stable complexes, and DM interaction partially collapses differences in dissociation rates. Thus, although disruption of conserved H bonds likely plays a role in DM action, DM apparently does not act exclusively by this mechanism but also alters sequence-dependent peptide/MHCII interactions, resulting in a binding site with diminished selectivity.

Importantly, both the comparison of LZ-stabilized DM/DR1 complexes with CLIP and HA and the average relationship between intrinsic stability and DM suscepti-

Table 1. Kinetic Parameters for Spontaneous and LZ-DM-Catalyzed Release of AMCA-HA and AMCA-CLIP from LZ-DR1

Parameter	AMCA-HA	AMCA-CLIP	CLIP/HA Ratio
k_{in}, no DM (s^{-1})[a]	2.98 ($\pm$ 1.13) $\times 10^{-7}$ (n = 15)	5.66 ($\pm$ 0.78) $\times 10^{-5}$ (n = 18)	192
$t_{1/2}$, no DM	30.3 d	3.5 hr	
k_d, 1:1 DM:pep/DR[b]	0.5 $\times 10^{-2}$	7.4 $\times 10^{-2}$	15
$t_{1/2}$, equimolar	142 s	9.4 s	
Fold DM effect	16,000$\times$	1300$\times$	
k_{cat} (s^{-1})[c]	1.2 ($\pm$ 0.66) $\times 10^{-2}$ (n = 3)	8.1 ($\pm$ 0.2) $\times 10^{-2}$ (n = 2)	6.9
$t_{1/2}$, Michaelis-Menten	60 s	8.6 s	
Fold DM effect	40,000$\times$	1400$\times$	
K_M (M)[c]	4.7 ($\pm$ 1.1) $\times 10^{-8}$ (n = 3)	9.2 ($\pm$ 0.4) $\times 10^{-8}$ (n = 2)	2.0

[a] Spontaneous off rates (k_{in}) and half-lives ($t_{1/2} = \ln(2)/k_{in}$) for AMCA-HA and -CLIP complexes with LZβ-DR1 in the absence of LZβ-DM were determined by fitting data to single-exponential decay models (Figure 6A). For HA, initial dissociations were tracked over 1–4 days; derived rate constants were independent of initial concentration (data not shown). A >3-week dissociation curve showed comparable kinetics; a fraction of the complexes may dissociate even more slowly (data not shown). Rates of AMCA-HA release from soluble DR1 without LZ domains were similar (1.8–3.5 $\times 10^{-7}$ s^{-1}, n = 2). Lower stability was reported previously for AMCA-HA bound to *E. coli*-derived soluble DR1 (Zarutskie et al., 2001) and for related HA peptides at pH 5 or 7 (Sloan et al., 1995; Roche and Cresswell, 1990; Joshi et al., 2000; Stratikos et al., 2002). Different sources of DR, structures of peptide analogs, assay conditions, and control of proteolysis may all contribute to the discrepancies.
[b] Off rates, k_d, for 1:1 complexes between AMCA-peptide/LZβ-DR1 and LZβ-DM were determined from the fast phase of the dissociation curves shown in Figures 6B and 6C. Each complex was analyzed twice with similar results.
[c] K_M and k_{cat} were determined by nonlinear least-squares fit of initial off rates to a Michaelis-Menten model, Rate = k_{cat} [DM] [DR/peptide]/(K_M + [DR/peptide]) (Figure 6E). Note that K_M values for AMCA-HA and AMCA-CLIP were similar, even though in previous studies, DM coprecipitated better with MHC II molecules carrying loosely bound peptides such as CLIP (Kropshofer et al., 1997; Denzin et al., 1996; R.B. and H.M. Scott, unpublished data). The latter results may reflect better DM association with empty MHC II molecules generated by release of peptide during the experiment, rather than with the peptide/DR complexes themselves; in contrast, K_M measures DM's affinity for the intact complex.

bility for multiple soluble peptide/DR2 or DR4 complexes show a common quantitative relationship: an ~100-fold difference in intrinsic stability is associated with only an ~10-fold difference in DM susceptibility. This strongly suggests that the common trend reflects a genuine property of DM/DR interactions rather than an artifact of the particular system used.

If DM can dissociate extremely stable peptide/MHCII complexes and presented peptides are not absolutely DM resistant, how are peptides selected for presentation? The exposure to DM in endosomes is very likely longer (Marsh et al., 1992; Guerra et al., 1998) than the 1–2 min $t_{1/2}$ of DM/DR1/HA, arguing that the DM effect is not regulated primarily by endosomal transit time. Instead, DM and MHCII levels may be modulated to ensure efficient CLIP release while avoiding excessive editing of stable peptides. DM expression is substoichiometric in peptide loading compartments (Ramachandra et al., 1996; Schafer et al., 1996; Glazier et al., 2002). Further, most DM molecules may be engaged in stabilizing empty molecules, rather than in peptide editing (Denzin et al., 1996). Under these conditions, quantitative differences in DM susceptibility may determine the fate of particular peptide/MHCII complexes. DM susceptibility is modestly correlated with increased intrinsic stability, but other undefined factors contribute (Belmares et al., 2002). The rules governing DM susceptibility will need to be elucidated for a full understanding of immunodominance.

Experimental Procedures

Cells

The Epstein-Barr virus (EBV)-transformed B cell line, 8.1.6, is *DR/DQ/DMB*-hemizygous but harbors two copies of *DMA*; its derivative, 9.5.3, lacks expression of DMβ (Morris et al., 1994); the related mutant 2.2.93 (gift of S. Fling, Corixa Corporation, Seattle, WA) lacks DMα (Fling et al., 1994). The 8.1.6 derivative, 5.2.4, has an additional deletion spanning the entire MHC on the other chromosome; the only expressed MHCII allele is DP4 (Mellins et al., 1991; Morris et al., 1994). 5.2.4/DR3 transfectants have been described (Doebele et al., 2000). ϕNX-A is a retroviral vector packaging line (Kinsella and Nolan, 1996). S2 *D. melanogaster* transfectants expressing soluble, full-length, and LZ-fused DM and DR molecules have been described (Sloan et al., 1995; Busch et al., 2002; Hall et al., 2002).

cDNA Constructs and Transfection

Wild-type cDNAs for *DMA**0101 and *DMB**0101 were PCR amplified with *Pfu* polymerase from pRM-*DMA* and pRM-*DMB* (gift of D. Zaller, Merck Research Laboratories, Rahway, NJ), using the primers, *DMA*-U1 (GGGTTGGGATCCCCTACCTACTGTGTGGCAAGA) and *DMA*-L1 (CCTCTGGAATTCTGGCCGAAGCTGCTGGCATCA) for *DMA*, *DMB*-U1 (GACTGAGAATTCGGCATCTTTACAGAGCAGAGC) and *DMB*-L1 (CATCATGTCGACTTGAATCTCCTTCTCACTTGG) for *DMB*. PCR products were cloned into retroviral pBMN-IRES vectors containing neomycin (Neo) or blasticidin (Blasti) resistance genes (Kitamura et al., 1995), using primer-encoded restriction sites. Random mutagenesis was done by error-prone PCR (Doebele et al., 2000); mutant *DMA* and *DMB* libraries (~10^5 colonies each) were subcloned into pBMN-IRES vectors. Eleven to twelve random clones from each library were sequenced to determine mutation rates. Based on the Poisson distribution, 34% *DMA* and 29% of *DMB* clones contained single point mutations. All possible single mutations were represented 46- and 36-fold in the *DMA* and *DMB* library, respectively.

Site-directed mutagenesis was done by overlap extension PCR using *Pfu* polymerase. Mutant cDNAs, cloned into pBMN-IRES-Neo (for *DMB*) and pBMN-IRES-Blasti (for *DMA*), were sequenced and 20 μg (for libraries) or 8 μg (for site-directed mutants) were transfected into EBV B cells as described (Doebele et al., 2000).

Construction, insect cell expression, and purification of soluble DM and DR1 molecules, fused to complementary AcidP1 and BaseP1 LZ domains via their β chain C termini (LZβ-DM and LZβ-DR1, respectively) were as described (Busch et al., 2002). A truncated *DRA* cDNA (α1 and α2 domains) was similarly fused at the C terminus

to the BaseP1 zipper via an 8 amino acid spacer (GGGSGGGS) and expressed in S2 cells with soluble *DRB1*0101* cDNA, and the LZα-DR1 molecules were purified by affinity chromatography.

Generation and Characterization of DM Mutant Cells

Drug-resistant 8.1.6 cells harboring mutant DM libraries were FACS sorted for elevated CLIP, and the brightest 0.5%–1% cells were cloned at one cell/well. Clones were expanded and rescreened by FACS for surface CLIP and total DR αβ dimers, using CerCLIP.1 (Avva and Cresswell, 1994) and L243 (Lampson and Levy, 1980), respectively. Mutant DM cDNAs were rescued by RT-PCR and sequenced. Single point mutations were created for random mutants with multiple mutations. Site-directed mutants were retrovirally transduced into 2.2.93 (for *DMA* mutants) and 9.5.3 (for *DMB* mutants). Drug-resistant polyclonal populations grown in 1 mg/ml G418 (Life Technologies, Grand Island, NY) or 2–4 μg/ml blasticidin S HCl (Calbiochem, San Diego, CA) were screened for elevated CLIP. To analyze surface DP4 levels, cells were stained with B7/21.2 (Robbins et al., 1987).

DM expression was measured in cell extracts (5×10^6 cells in buffer containing 1% IGEPAL CA-640), by immunoprecipitation using 47G.S4 (Schafer et al., 1996). Precipitates were titrated, resolved by SDS-PAGE, and transferred to PVDF membranes; DMβ-associated α chains were detected by mAb 5C1 (Sanderson et al., 1996) and quantified using GS110 densitometer and QuantityOne software (Bio-Rad Laboratories). A linear range was established for titrated wt extract on each film, and each dilution of the mutant giving a signal within this range was used to calculate mutant DM expression relative to wt. Analyses were considered valid only if similar values were obtained at a minimum of two dilutions. In addition, cells were permeabilized with Cytofix/Cytoperm (BD Pharmingen, San Diego), stained with MaP.DM1-PE (Denzin et al., 1997; BD Pharmingen), and analyzed by FACS. For analysis of DM/DO association, DO was immunoprecipitated with rabbit anti-DOβ cytoplasmic tail serum, raised against KLH-coupled synthetic CRAQK GYVRTQMSGNEVSRAVLLPQS peptide; Cocalico Biologicals, Reamstown, PA) and detected by immunoblot using DOB.L1 (BD Pharmingen); associated DM was detected using 5C1.

In Vitro Assays of DM/DR Interaction

DM was immunoprecipitated from titrated extracts of EBV B cells, using 47G.S4. An aliquot of each precipitate was blotted for DM recovery. Another was added to full-length DR*0402 (1% insect cell lysate; ~10 nM) plus 20-40 μg/ml Bio-HCgp39 (262-276) peptide (Hall et al., 2002) or to 10 nm full-length DR3 and Bio-CLIP (81–99) in buffer: 50 mM sodium acetate (pH 4.7), 150 mM NaCl, 0.5% IGEPAL, 1% BSA, 0.05% NaN_3, and complete protease inhibitors (Roche Diagnostics, Mannheim, Germany). After incubation (37°C, 2–4 hr), the reaction was stopped using buffer with 50 mM Tris-Cl (pH 8.2) at 4°C. Peptide/DR complexes were quantified by L243 capture on ELISA plates, development with streptavidin-Eu^{3+}, and time-resolved fluorescence analysis (Sloan et al., 1995). Similarly, we quantified the ability of LZβ-DM or soluble DM (sDM) to promote binding of 10 μM Bio-HA (306–318) peptide (Lamb et al., 1982) to purified 10 nM sDR1 or LZ-modified DR1 in a 3 hr reaction at pH 4.7 (Busch et al., 2002) or 7.0 (50 mM sodium phosphate instead of acetate). LZ-mediated DM/DR binding was tested by mixing both molecules, immunoprecipitating with 2H11 (Chang et al., 1994) or normal mouse Ig, and immunoblotting with CHAMP and 5C1, as described (Busch et al., 2002).

Kinetic Measurements

For real-time dissociation experiments, we incubated AMCA-labeled variant HA or CLIP peptides (Joshi et al., 2000) (ca. 100 μM) overnight with LZβ-DR1 (1–10 μM) at 37°C in buffer (10 mM sodium phosphate/100 mM sodium citrate [pH ~5.1], 150 mM NaCl, 0.05% Tween 20, 0.02% NaN_3, 20 μg/ml leupeptin, 1 mM PMSF, 2 μg/ml TLCK, 5 mM EDTA). Free peptide was removed using Sephadex G50 superfine spin columns. The integrity of the LZβ-DR1 molecules after loading was checked by immunoblotting using the anti-DR antiserum, CHAMP (Stern and Wiley, 1992). Complexes were diluted in assay buffer and allowed to dissociate at 37°C in the presence of 67–100 μM unlabeled HA (306–318) peptide, with or without LZβ-DM. Dissociations were performed in black, flat-bottom 96-well polypropylene plates (Greiner, Longwood, FL) sealed with UV-transparent tape (VIEWseal, Greiner) for longer experiments. Fluorescence was recorded with excitation at 280 and 354 nm and emission at 450 nm, using a Gemini XS multiwell fluorometer (Molecular Devices, Sunnyvale, CA). The ratio of background-subtracted FRET fluorescence ($F_{280\rightarrow450}$) to AMCA fluorescence ($F_{354\rightarrow450}$) was ~0.2 for free and ~1.45 for bound peptide, allowing estimation of the fraction of bound peptide. For Michaelis-Menten kinetics, peptide/DR complexes were quantified by AMCA fluorescence, standardized against a known amount of AMCA peptide (Joshi et al., 2000).

To measure susceptibility of peptide/soluble DR complexes to soluble DM, dissociation of fluoresceinated peptides from DR was followed using a size exclusion chromatography assay (Belmares et al., 2002). Except for the absence of Tween and protease inhibitors, conditions were similar to those in the real-time FRET assay. Single-exponential dissociation rate constants, k_{obs} and k_{in}, were determined in the presence or absence of 0.25 μM DM, respectively, and used to calculate j, a measure of DM susceptibility, using the relationship, $k_{obs} = k_{in} + j\, k_{in}\, [DM]$ (Weber et al., 1996).

Acknowledgments

We thank C.W. Townsley for protein purification, Drs. S. Fling, L. Karlsson, G. Sonderstrup, L. Stern, and D. Zaller for reagents, and Drs. H. McConnell and T. Anderson for discussions. The work was supported in part by the NIH (RO1-AI28809 to E.D.M.), the Siegelman fellowship (to R.B.), and a Cancer Research Institute fellowship (to A.P.).

Received: September 10, 2002
Revised: April 7, 2003
Accepted: April 9, 2003
Published: August 19, 2003

References

Avva, R.R., and Cresswell, P. (1994). In vivo and in vitro formation and dissociation of HLA-DR complexes with invariant chain-derived peptides. Immunity *1*, 763–774.

Belmares, M.P., Busch, R., Wucherpfennig, K.W., McConnell, H.M., and Mellins, E.D. (2002). Structural factors contributing to DM susceptibility of MHC class II/peptide complexes. J. Immunol. *169*, 5109–5117.

Burmeister, W.P., Gastinel, L.N., Simister, N.E., Blum, M.L., and Bjorkman, P.J. (1994). Crystal structure at 2.2 Å resolution of the MHC-related neonatal Fc receptor. Nature *372*, 336–343.

Busch, R., and Mellins, E.D. (1996). Developing and shedding inhibitions: how MHC class II molecules reach maturity. Curr. Opin. Immunol. *8*, 51–58.

Busch, R., Reich, Z., Zaller, D.M., Sloan, V., and Mellins, E.D. (1998). Secondary structure composition and pH-dependent conformational changes of soluble recombinant HLA-DM. J. Biol. Chem. *273*, 27557–27564.

Busch, R., Pashine, A., Garcia, K.C., and Mellins, E.D. (2002). Stabilization of soluble, low-affinity HLA-DM/HLA-DR1 complexes by leucine zippers. J. Immunol. Methods *263*, 111–121.

Chang, H.C., Bao, Z., Yao, Y., Tse, A.G., Goyarts, E.C., Madsen, M., Kawasaki, E., Brauer, P.P., Sacchettini, J.C., Nathenson, S.G., et al. (1994). A general method for facilitating heterodimeric pairing between two proteins: application to expression of α and β T-cell receptor extracellular segments. Proc. Natl. Acad. Sci. USA *91*, 11408–11412.

Chou, C.L., and Sadegh-Nasseri, S. (2000). HLA-DM recognizes the flexible conformation of major histocompatibility complex class II. J. Exp. Med. *192*, 1697–1706.

Denzin, L.K., Hammond, C., and Cresswell, P. (1996). HLA-DM interactions with intermediates in HLA-DR maturation and a role for HLA-DM in stabilizing empty HLA-DR molecules. J. Exp. Med. *184*, 2153–2165.

Denzin, L.K., Sant'Angelo, D.B., Hammond, C., Surman, M.J., and

Cresswell, P. (1997). Negative regulation by HLA-DO of MHC class II-restricted antigen processing. Science *278*, 106–109.

Doebele, R.C., Busch, R., Scott, H.M., Pashine, A., and Mellins, E.D. (2000). Determination of the HLA-DM Interaction Site on HLA-DR Molecules. Immunity *13*, 517–527.

Faubert, A., Samaan, A., and Thibodeau, J. (2002). Functional analysis of tryptophans α62 and β120 on HLA-DM. J. Biol. Chem. *277*, 2750–2755.

Fling, S.P., Arp, B., and Pious, D. (1994). HLA-*DMA* and -*DMB* genes are both required for MHC class II/peptide complex formation in antigen-presenting cells. Nature *368*, 554–558.

Fremont, D.H., Crawford, F., Marrack, P., Hendrickson, W.A., and Kappler, J. (1998). Crystal structure of mouse H2-M. Immunity *9*, 385–393.

Gao, G.F., Tormo, J., Gerth, U.C., Wyer, J.R., McMichael, A.J., Stuart, D.I., Bell, J.I., Jones, E.Y., and Jakobsen, B.K. (1997). Crystal structure of the complex between human CD8α (α) and HLA-A2. Nature *387*, 630–634.

Glazier, K.S., Hake, S.B., Tobin, H.M., Chadburn, A., Schattner, E.J., and Denzin, L.K. (2002). Germinal center B cells regulate their capability to present antigen by modulation of HLA-DO. J. Exp. Med. *195*, 1063–1069.

Guerra, C.B., Busch, R., Doebele, R.C., Liu, W., Sawada, T., Kwok, W.W., Chang, M.D., and Mellins, E.D. (1998). Novel glycosylation of HLA-DRα disrupts antigen presentation without altering endosomal localization. J. Immunol. *160*, 4289–4297.

Hall, F., Rabinowitz, J., Busch, R., Visconti, K., Belmares, M., Patil, N., Cope, A., Patel, S., McConnell, H., Mellins, E., et al. (2002). Relationship between kinetic stability and immunogenicity of HLA-DR4/peptide complexes. Eur. J. Immunol. *32*, 662–670.

Joshi, R.V., Zarutskie, J.A., and Stern, L.J. (2000). A three-step kinetic mechanism for peptide binding to MHC class II proteins. Biochemistry *39*, 3751–3762.

Kinsella, T.M., and Nolan, G.P. (1996). Episomal vectors rapidly and stably produce high-titer recombinant retrovirus. Hum. Gene Ther. *7*, 1405–1413.

Kitamura, T., Onishi, M., Kinoshita, S., Shibuya, A., Miyajima, A., and Nolan, G.P. (1995). Efficient screening of retroviral cDNA expression libraries. Proc. Natl. Acad. Sci. USA *92*, 9146–9150.

Kropshofer, H., Arndt, S.O., Moldenhauer, G., Hämmerling, G.J., and Vogt, A.B. (1997). HLA-DM acts as a molecular chaperone and rescues empty HLA-DR molecules at lysosomal pH. Immunity *6*, 293–302.

Kropshofer, H., Vogt, A.B., Thery, C., Armandola, E.A., Li, B.C., Moldenhauer, G., Amigorena, S., and Hämmerling, G.J. (1998). A role for HLA-DO as a co-chaperone of HLA-DM in peptide loading of MHC class II molecules. EMBO J. *17*, 2971–2981.

Lamb, J.R., Eckels, D.D., Phelan, M., Lake, P., and Woody, J.N. (1982). Antigen-specific human T lymphocyte clones: viral antigen specificity of influenza virus-immune clones. J. Immunol. *128*, 1428–1432.

Lampson, L.A., and Levy, R. (1980). Two populations of Ia-like molecules on a human B cell line. J. Immunol. *125*, 293–299.

Liljedahl, M., Kuwana, T., Fung-Leung, W.P., Jackson, M.R., Peterson, P.A., and Karlsson, L. (1996). HLA-DO is a lysosomal resident which requires association with HLA-DM for efficient intracellular transport. EMBO J. *15*, 4817–4824.

Marsh, E.W., Dalke, D.P., and Pierce, S.K. (1992). Biochemical evidence for the rapid assembly and disassembly of processed antigen-major histocompatibility complex class II complexes in acidic vesicles of B cells. J. Exp. Med. *175*, 425–436.

McFarland, B.J., and Beeson, C. (2002). Binding interactions between peptides and proteins of the class II major histocompatibility complex. Med. Res. Rev. *22*, 168–203.

Mellins, E., Kempin, S., Smith, L., Monji, T., and Pious, D. (1991). A gene required for class II-restricted antigen presentation maps to the major histocompatibility complex. J. Exp. Med. *174*, 1607–1615.

Morris, P., Shaman, J., Attaya, M., Amaya, M., Goodman, S., Bergman, C., Monaco, J.J., and Mellins, E. (1994). An essential role for HLA-DM in antigen presentation by class II major histocompatibility molecules. Nature *368*, 551–554.

Mosyak, L., Zaller, D.M., and Wiley, D.C. (1998). The structure of HLA-DM, the peptide exchange catalyst that loads antigen onto class II MHC molecules during antigen presentation. Immunity *9*, 377–383.

Raddrizzani, L., Bono, E., Vogt, A.B., Kropshofer, H., Gallazzi, F., Sturniolo, T., Hämmerling, G.J., Sinigaglia, F., and Hammer, J. (1999). Identification of destabilizing residues in HLA class II-selected bacteriophage display libraries edited by HLA-DM. Eur. J. Immunol. *29*, 660–668.

Ramachandra, L., Kovats, S., Eastman, S., and Rudensky, A.Y. (1996). Variation in HLA-DM expression influences conversion of MHC class II αβ:class II-associated invariant chain peptide complexes to mature peptide-bound class II alpha beta dimers in a normal B cell line. J. Immunol. *156*, 2196–2204.

Robbins, P.A., Evans, E.L., Ding, A.H., Warner, N.L., and Brodsky, F.M. (1987). Monoclonal antibodies that distinguish between class II antigens (HLA- DP, DQ, and DR) in 14 haplotypes. Hum. Immunol. *18*, 301–313.

Roche, P.A., and Cresswell, P. (1990). High-affinity binding of an influenza hemagglutinin-derived peptide to purified HLA-DR. J. Immunol. *144*, 1849–1856.

Sanderson, F., Thomas, C., Neefjes, J., and Trowsdale, J. (1996). Association between HLA-DM and HLA-DR in vivo. Immunity *4*, 87–96.

Schafer, P.H., Green, J.M., Malapati, S., Gu, L., and Pierce, S.K. (1996). HLA-DM is present in one-fifth the amount of HLA-DR in the class II peptide-loading compartment where it associates with leupeptin-induced peptide (LIP)-HLA-DR complexes. J. Immunol. *157*, 5487–5495.

Siklodi, B., Vogt, A.B., Kropshofer, H., Falcioni, F., Molina, M., Bolin, D.R., Campbell, R., Hämmerling, G.J., and Nagy, Z.A. (1998). Binding affinity independent contribution of peptide length to the stability of peptide-HLA-DR complexes in live antigen presenting cells. Hum. Immunol. *59*, 463–471.

Sloan, V.S., Cameron, P., Porter, G., Gammon, M., Amaya, M., Mellins, E., and Zaller, D.M. (1995). Mediation by HLA-DM of dissociation of peptides from HLA-DR. Nature *375*, 802–806.

Stern, L.J., and Wiley, D.C. (1992). The human class II MHC protein HLA-DR1 assembles as empty α β heterodimers in the absence of antigenic peptide. Cell *68*, 465–477.

Stratikos, E., Mosyak, L., Zaller, D.M., and Wiley, D.C. (2002). Identification of the lateral interaction surfaces of human histocompatibility leukocyte antigen (HLA)-DM with HLA-DR1 by formation of tethered complexes that present enhanced HLA-DM catalysis. J. Exp. Med. *196*, 173–183.

Tormo, J., Natarajan, K., Margulies, D.H., and Mariuzza, R.A. (1999). Crystal structure of a lectin-like natural killer cell receptor bound to its MHC class I ligand. Nature *402*, 623–631.

Ullrich, H.J., Doring, K., Gruneberg, U., Jahnig, F., Trowsdale, J., and van Ham, S.M. (1997). Interaction between HLA-DM and HLA-DR involves regions that undergo conformational changes at lysosomal pH. Proc. Natl. Acad. Sci. USA *94*, 13163–13168.

Weber, D.A., Evavold, B.D., and Jensen, P.E. (1996). Enhanced dissociation of HLA-DR-bound peptides in the presence of HLA-DM. Science *274*, 618–620.

Weber, D.A., Dao, C.T., Jun, J., Wigal, J.L., and Jensen, P.E. (2001). Transmembrane domain-mediated colocalization of HLA-DM and HLA-DR is required for optimal HLA-DM catalytic activity. J. Immunol. *167*, 5167–5174.

Zarutskie, J.A., Busch, R., Zavala-Ruiz, Z., Rushe, M., Mellins, E.D., and Stern, L.J. (2001). The kinetic basis of peptide exchange catalysis by HLA-DM. Proc. Natl. Acad. Sci. USA *98*, 12450–12455.